Polymer Testing 86 (2020) 106478

Contents lists available at ScienceDirect

Polymer Testing

journal homepage: www.elsevier.com/locate/polytest

A comprehensive thermo-viscoelastic experimental investigation of Ecoflex polymer

Zisheng Liao [a,b], Mokarram Hossain [b,*], Xiaohu Yao [a,c,**], Rukshan Navaratne [d], Gregory Chagnon [e]

[a] School of Civil Engineering and Transportation, South China University of Technology, 510640 Guangzhou, Guangdong, China
[b] Zienkiewicz Centre for Computational Engineering, College of Engineering, Swansea University, SA1 8EN, United Kingdom
[c] State Key Laboratory of Subtropical Building Science, South China University of Technology, 510640 Guangzhou, China
[d] Aerospace Engineering Department, University of South Wales, Pontypridd, Cardiff, United Kingdom
[e] University of Grenoble Alpes, CNRS, Grenoble INP, TIMC-IMAG, F-38000 Grenoble, France

ARTICLE INFO

Keywords:
Ecoflex silicone rubber
Mullins effect
Stress recovery
Strain rate dependence
Temperature dependence

ABSTRACT

Silicone polymers have enormous applications, especially in the areas of biomedical engineering. Ecoflex, a commercially available room temperature cured silicone polymer, has attracted considerable attention due to its wide range of applications as medical-grade silicones and as matrix materials in producing nano-filled stretchable sensors and dielectric elastomers for soft robotics. In this contribution, we have conducted a wide range of experiments under thermo-mechanical loadings. These experiments consist of loading–unloading cyclic tests, single-step relaxation tests, Mullins effects tests at different strain rates and stretches, stress recovery tests at different rest time, etc. In order to assess the temperature influences on Ecoflex, a number of viscoelastic tests are performed in a thermal chamber with temperature ranging from -40°C to 140°C. Extensive experimental findings illustrate that Ecoflex experiences a significant stress softening in the first cycles and such a softening recovers gradually with respect to time. It also shows a significant amount of cyclic dissipations at various stretch levels as well as a considerable stress relaxation only for virgin samples. Cyclic dissipations and stress relaxation almost disappear for the case of pre-stretched samples. Furthermore, the material is more or less sensitive under a wide range of temperature differences.

1. Introduction

Many silicone polymers have promising properties, such as bio-compatibility, good transparency, non-toxicity, good dielectric properties, high hydrophobicity, thermal stability, good processability, climate, oxidative, and UV resistances. Another aspect of silicones is that they do not react with most chemicals. Good bio-compatibility and relatively inert actions with chemicals make them one of the most crucial engineering materials especially in biomedical applications, e.g., for tubing, peristaltic pumps, catheters and cardiovascular devices such as heart pumps, ventricular assist devices, cannulas and vascular grafts [1–5]. Furthermore, RTV (Room Temperature Vulcanization) silicones have been used for skin-like applications or external maxillofacial prosthetics [5]. As their stiffness values match those attributed to compliant biological tissues, silicone polymers are massively used as substrates in mechanobiology. In addition to processability, transparency and non-toxicity, the possibility of relatively easy tuning of the mechanical properties of silicones by changing the polymer to curing agent ratio, or curing conditions is an attractive feature. These properties offer further advantages which favour the application of silicone-based elastomers in dynamic bioreactors and experimental devices for mechanobiological studies. Note that the applications of silicones are not limited to biomedical engineering. They are one of the key materials in recently emerging soft robotics [1]. Thanks to many promising rheological and mechanical properties such as low viscosity, high reproducibility, large deformability, low sensitivity to temperature, silicone-inspired filled polymers are major candidates in flexible stretch-sensors for healthcare applications, actuators in soft robotics and flexible materials for energy harvesting from ambient motions such as human walking and ocean and tidal waves [1,6]. Moreover, due to low dissipative behaviour and low leakages characteristics, silicones and their composites have a wide range of applications in aerospace industries [7].

Very recently, a commercially available silicone rubber, Ecoflex (Smooth-On, USA), becomes a typical elastomer for a wide range of

* Corresponding author.
** Corresponding author at: School of Civil Engineering and Transportation, South China University of Technology, 510640 Guangzhou, Guangdong, China.
E-mail addresses: l.zisheng@mail.scut.edu.cn (Z. Liao), mokarram.hossain@swansea.ac.uk (M. Hossain), yaoxh@scut.edu.cn (X. Yao), rukshan.navaratne@southwales.ac.uk (R. Navaratne), gregory.chagnon@univ-grenoble-alpes.fr (G. Chagnon).

https://doi.org/10.1016/j.polymertesting.2020.106478
Received 13 January 2020; Accepted 5 March 2020
Available online 10 March 2020

practical applications. The two component room temperature curable silicone comes up with several Shore hardnesses ranging from Shore 00-10 to Shore 00-65. Strain sensors as epidermal electronic systems have widely been used nowadays where the mechanical compliance like human skin and a high stretchability are required. Due to low viscosities, high medical-grade, high reproducibility, silicone elastomers and their composites are ideal candidates in the area of flexible stretch-based sensors. Amjadi et al. [8] made a super-stretchable, skin-mountable, and ultra-soft strain sensors by using Ecoflex-carbon nanotube nanocomposite thin films. They demonstrated that Ecoflex-based soft materials, where the sensing is enhanced by carbon nanotubes, have excellent hysteresis performance at different strain levels and rates with a high linearity and a small drift. Deep tissue injury caused by a prolonged mechanical loading disrupts blood flow and metabolic clearance. In order to mimic stress and strain in deep muscle tissues, the ability of Ecoflex is rigorously studied by Sparks et al. [9]. In this case, they conducted unconfined compression experiments on two different Shores, i.e., Ecoflex Shore 00-10 and Shore 00-30. The design of the actuation system is based on three fluidic chambers equally spaced in radial arrangement embedded in an Ecoflex matrix (Shore 00-50).

Despite increasing applications of Ecoflex in recent years, to the best of the authors' knowledge, a comprehensive thermo-viscoelastic investigation consisting of some critical experimentations, that are essential to quantify a typical viscoelastic material, are absent in the literature. Hence, in this study, we perform loading–unloading–reloading cyclic tests at different strain rates and strain levels, single-step relaxation tests with various strains and holding time, stress softening tests for identifying Mullins effect, etc. These tests are conducted at various temperature profiles ranging from −40 °C to 140 °C. Since the material shows a significant stress recovery with time, a detailed study on the time-dependent stress recovery is presented. In contrast to other classical silicone polymers, Ecoflex shows some temperature-sensitive responses. The material shows a significant dissipative behaviour when tests are performed on virgin specimens. However, these dissipations are quickly disappeared in the case of repeated cycles. The same phenomenon is observed in single-step relaxation tests where virgin samples demonstrate pronounced viscous or recoverable non-equilibrium stresses. However, they are diminished once tests are conducted on pre-treated samples. Moreover, the material shows no residual strain upon reloading as well as it can recover stress softening almost fully after a sufficiently long period of time.

The paper is organized as follows: in Section 2 a brief description is presented to outline the experimental set-up, procedures for sample preparations which are utilized to perform the experiments in our laboratory. In the following section Section 3, comprehensive experimental results are illustrated in detail, and sufficient analyses are given. In these cases, cyclic and relaxation behaviour of Ecoflex are extensively analysed. Furthermore, the strain rate and temperature dependencies of the polymer are investigated and explained in the same section. Finally, section Section 4 summarizes all major findings obtained in the study.

2. Experimental details

2.1. Specimen preparation

In this paper, Ecoflex™ silicone rubber of hardness Shore 00-30 is adopted for experimental investigations. Ecoflex is a platinum-catalyzed silicone mixed by two parts of liquid ingredients. In order to produce specimens in the desired shape, a mould is produced using a photosensitive resin with the help of a 3D printer. The mould is shown in Fig. 1. For uniaxial type tensile tests, rectangular specimens with 50 mm × 5 mm × 1 mm (length × width × thickness) are adopted mainly. Similar dimensions were chosen in previous experimental studies of various soft polymers in the case of uniaxial tensile tests, see [10–14]. However, for tests inside the temperature chamber, due to the displacement constraint, 40 mm length specimens are adopted where specimens can be stretched maximally up to strain 400%.

Fig. 1. A 3D printed mould for sample preparation.

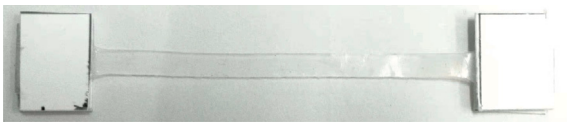

Fig. 2. A typical specimen of 50 mm × 5 mm × 1 mm size that is attached with two grippers.

To prepare Ecoflex samples, two liquid parts are mixed with a 1:1 ratio and stirred well. The liquid mixture is then injected to the mould cavities by a syringe to control the volume of specimens. Afterwards, an extra degassing is carried out in a vacuumiser to guarantee the removal of trapped air bubbles. As per specifications of the Ecoflex supplier (Smooth-On), the curing time of the two-component liquids should be four hours. However, we wait twelve hours so that specimens are fully cured into solid forms. Then they are demoulded smoothly. Note that Rey et al. [15] found in their investigations that specimens cured at room temperature were not fully crosslinked. Hence, they heated specimens at an elevated temperature for a certain time to obtain a better crosslinking. They observed that such a temperature-enhanced curing of some silicones resulted in increased mechanical properties. Therefore, in our study, some specimens are further cured at 80 °C for another four hours. Afterwards, we conduct a comparative study with samples cured under two different conditions. Results are presented in Section 3.1.

Note that due to extreme softness and stretchability of the Ecoflex polymer, the specimens show a tendency to slide out from the grippers. Therefore, before mounting to the test machine, both ends of every specimen are adhered to plastic slices using silicone glue in case a specimen slides out of the grippers, as is shown in Fig. 2.

2.2. Experimental set-up

Extensive and systematic experimental characterizations are carried out on the Ecoflex silicone by an Instron 5567 universal test machine.

For thermo-mechanical experimentations, the test machine is placed in a customized temperature chamber as shown in Fig. 3. A force sensor (④ in Fig. 3) of ±50 N maximum capacity with a precision of 0.001 N is used. Temperature can be regulated inside a chamber (③ in Fig. 3) from −50 °C to 150 °C. The maximum loading speed of the machine crosshead (⑤ in Fig. 3) is 8 mm/s. The displacement limit of the machine without using the temperature chamber is 800 mm, while the limit is confined to 200 mm within the chamber. A Bluehill® universal user interface software on the control computer (② in Fig. 3) is utilized to interact with the machine and to extract experimental data.

In this paper, all stress results are presented as the first Piola (nominal) stress (i.e., the applied force divided by the initial undeformed cross-sectional area) against the corresponding nominal strain (i.e., applied displacement divided by the initial length of the specimen). Strain rates, mentioned in this contribution, are the time derivative of the

Fig. 3. A complete thermo-viscoelastic testing system: ① is the main framework of the Instron 5567, ② is the control computer, ③ is the temperature chamber, ④ is the force sensor to monitor the applied force, and ⑤ is the crosshead of ①.

nominal strain. In order to ensure the reproducibility of obtained results, more than five samples of each test condition are carried out and an averaging technique is applied to find the best data set. At least two hundred data points of each test are acquired from the software. For tests conducted inside the temperature chamber, oscillations in the data (around ±0.003 MPa) are observed due to the specimen vibration caused by the air circulation as the Ecoflex polymer is extremely soft material. Therefore, smoothing techniques are applied to reduce such noises. Before testing, the specimen is mounted between the upper and lower grippers and regulated at the target temperature for thirty minutes if necessary. In the following sections, the experimental procedures and related results covering major characterization techniques on Ecoflex of hardness Shore 00-30 will be discussed in detail.

3. Experimental results

In this section, standard uniaxial tensile experimentations for thermo-viscoelastic characterization is performed on Ecoflex Shore 00-30. In addition, a variety of protocols of reloading tests are also conducted to investigate the softening and recovery features of the material. Furthermore, some typical characteristics of soft polymers such as strain rate and temperature dependence are also covered in our study.

This section is arranged as follows. At first, a few tests to verify the reproducibility and the independence of cure conditions are carried out in Section 3.1. In Section 3.2, a couple of cyclic tests is firstly performed to characterize the hysteresis and strain-induced stress softening behaviour. Afterwards, in Section 3.3, a set of single-step relaxation tests are conducted to show the time-dependent behaviour of the material. Then the relationship between the stress softening and the stress relaxation is discussed, and the concepts of equilibrium stress and non-equilibrium stress are put forward. Based on these concepts, in Section 3.5, tests at different strain rates are carried out to inspect the rate dependence on both portions of stresses and to discuss the possible existence of viscoelasticity. In addition, in Section 3.6, the influences of temperature on both portions are also discussed. Finally in Section 3.7, the stress recovery is rigorously investigated on stretched specimens after different recovery times. Apart from the temperature tests in Section 3.6, all tests in this section are carried out at ambient

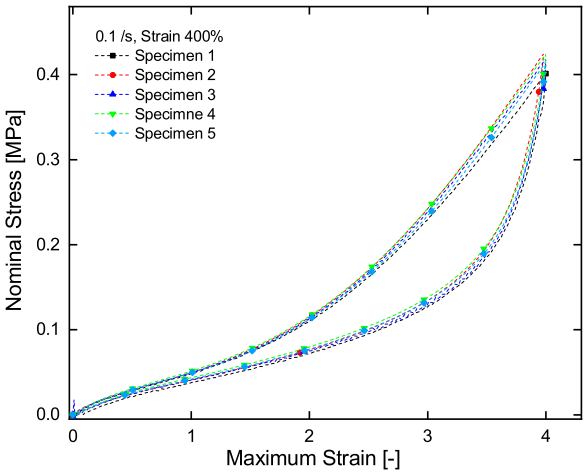

Fig. 4. Reproducibility of test samples: Several cyclic tests are conducted at strain 400% under the sample loading protocols.

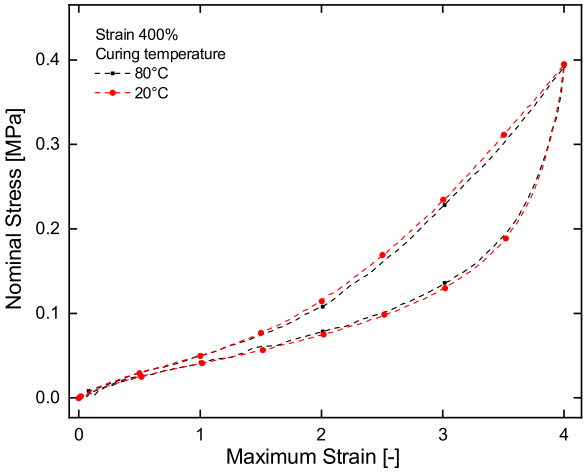

Fig. 5. Temperature dependency on Ecoflex curing: Cyclic tests at strain 400%; one cured at 20 °C and another cured at 80 °C.

temperature (20 °C). Furthermore, except the strain rate tests presented in Section 3.5, all tests are performed at a strain rate of 0.1/s.

3.1. Reproducibility tests

Prior to actual experiments, the reproducibility of material samples is verified by applying the same test protocol to at least five different specimens. From Fig. 4, it can be observed that only small fluctuations (less than 0.03 MPa difference at strain 400%) exist among manually produced specimens within an acceptable scale. As is mentioned above, to evaluate the influence of crosslinking effects at different temperatures, some specimens are additionally cured at 80 °C for four hours. Fig. 5 illustrates that the curing temperature does not have any considerable influence on the mechanical stress response.

3.2. Cyclic behaviour

In order to characterize the basic loading and unloading behaviour of Ecoflex (Shore 00-30), cyclic tests are performed on different specimens at strain levels of 100%, 200%, 300%, 400%, and 500%, respectively, with ten repeated cycles each. For all tests, a strain rate of 0.1/s is selected where the results are illustrated in Fig. 6.

Fig. 6(b) shows test the results of a sample at strain 400% with ten repeated loading–unloading cycles. On the primary loading path

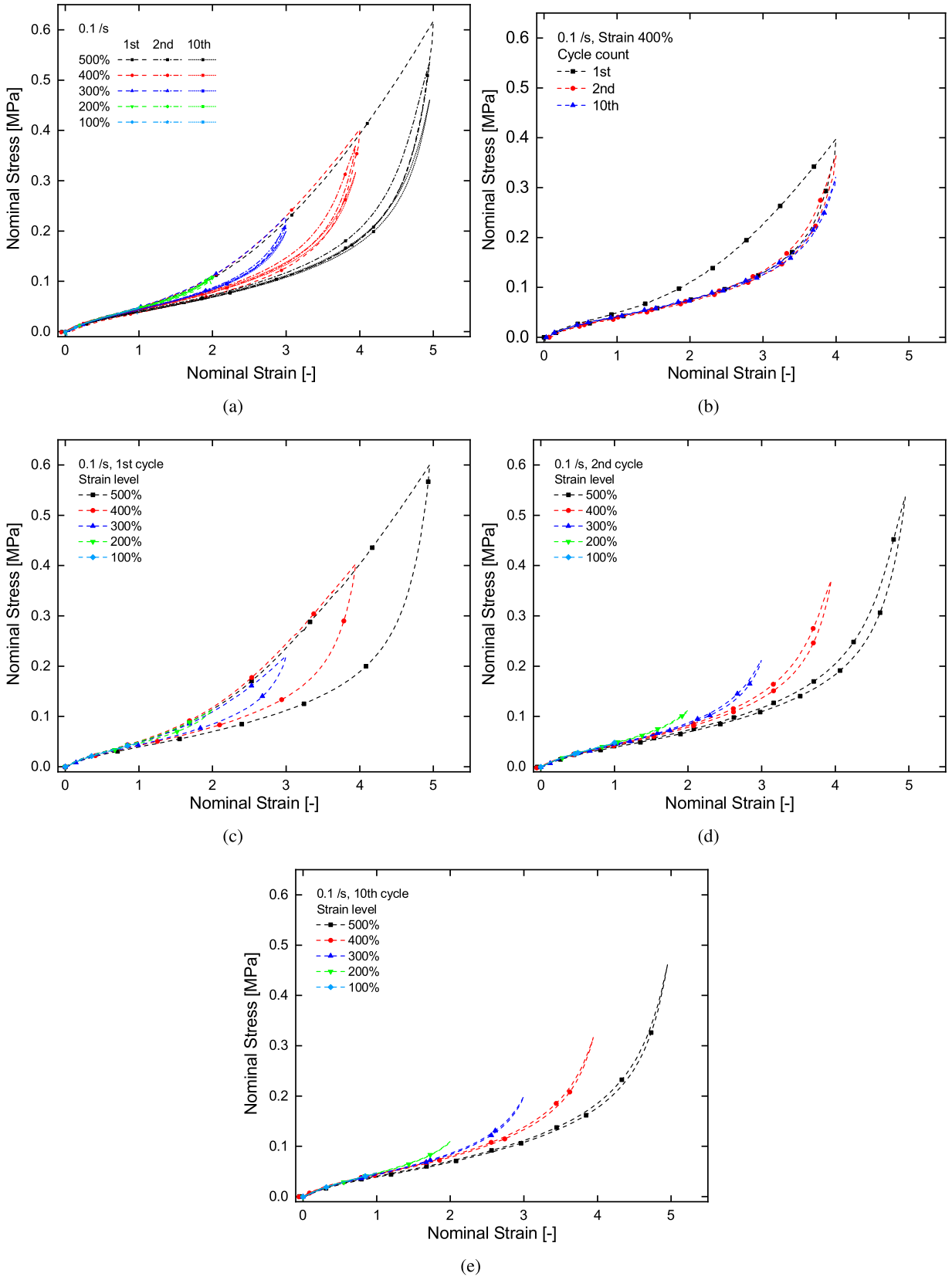

Fig. 6. Cyclic tests at five different strain levels. (a) Summary of all results for various cycles, (b) test results of a sample at strain 400% after ten repeated cycles, (c) only first cycles of tests at different strain levels, (d) the second cycles, (e) the tenth cycles.

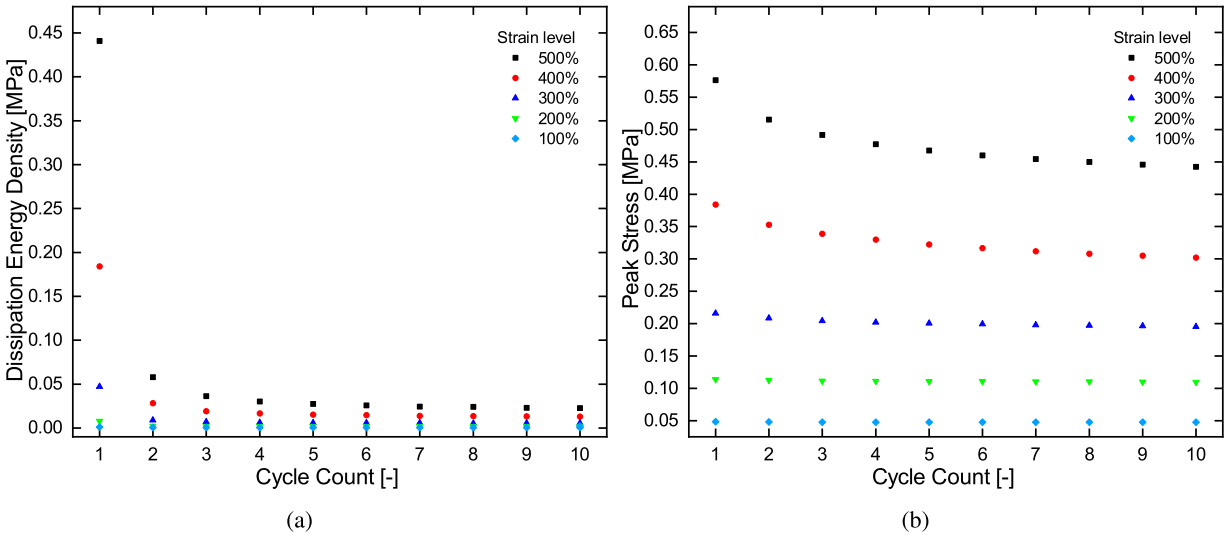

Fig. 7. Peak stress and dissipation energy density produced by cyclic tests at different strain levels with multiple cycles. (a) dissipation energy density versus cycle count, (b) peak stress versus cycle count.

(the black dash curve with square symbol), the material follows a typical nonlinear stress–strain behaviour on a virgin specimen (without any mechanical pre-treatments). The stiffness decreases slightly and stabilizes quickly at the beginning of the loading path. Afterwards, it transforms into an upturned pattern from strain 80%. Compared to the primary loading path, each reloading path in the second (the red dash curve with circle symbol) and the following cycles (e.g., the blue dash curve with triangle symbol) experiences an apparent stress reduction, and exhibits a stronger nonlinearity with an 'S' shape. The stiffness plateau extends significantly, and at a strain close to the maximum of the previous strain, stress increases rapidly and almost joins back to the primary curve, which is described as 'the strain hardening' [16]. The stress reduction behaviour is called the stress softening or the Mullins effect [35]. At the subsequent cycles after the first one, the softening still occurs, but it is insignificant compared to the first one and the responses between cycles and between loading and unloading paths tend to coincide. Note that before strain 100%, the stress softening is negligible. Figs. 6(c)–6(e) compare the first, the second, and the tenth cycles at different strains. From each figure, it can be seen that with a higher maximum strain level, the stress level in the unloading or the reloading path decreases progressively at a particular strain, indicating that the stress softening behaviour is a strain-induced phenomenon.

Fig. 7 illustrates the peak stress and hysteresis responses of the tests presented in Fig. 6. The stress softening behaviour causes a gap between the loading and unloading paths. This gap forms a hysteresis loop and contributes to the dissipation energy density w, which is calculated as the closed area inside the loading and unloading path l, i.e.,

$$w = \int_l \sigma \mathrm{d}\varepsilon, \tag{1}$$

where σ and ε are the nominal stress and nominal strain, respectively. The level of stress softening can be evaluated by the dissipation energy density. Fig. 7(a) clearly shows that the hysteresis decreases progressively with more cycles. The decrease mainly happens between the first and the second cycles, and stabilizes at a very low level soon in the subsequent cycles. Note that the hysteresis caused by the stress softening, i.e., the part that is removed in the subsequent cycles, and that caused by viscoelasticity, i.e, the part remains, should be distinguished. A tiny amount of hysteresis after ten cycles' at each strain level may indicate a minimal level of viscoelasticity. However, this is neither the main feature of Ecoflex polymer nor the primary response of the material. Fig. 7(b) plots the change of the peak stress (the stress at the maximum strain) with the cycle count. When a specimen is reloaded

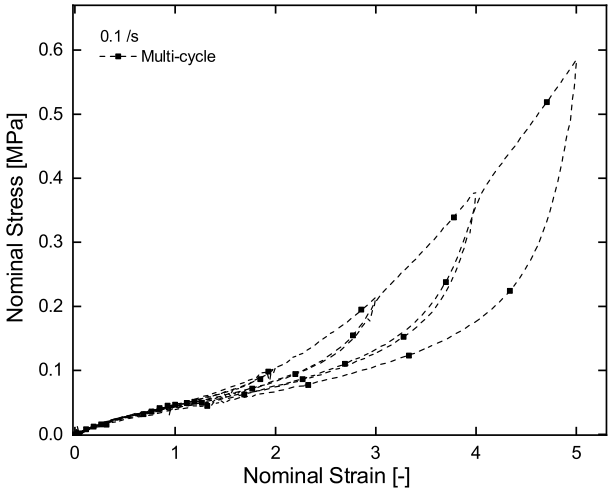

Fig. 8. A multiple cyclic test with increasing strain levels.

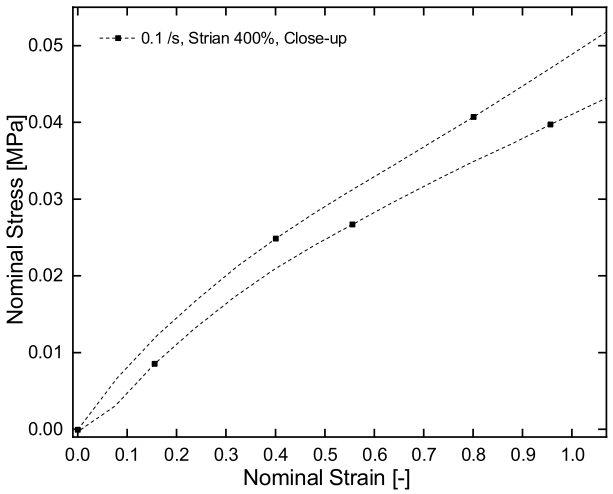

Fig. 9. A zoom-in graph for a cyclic test at strain 400%.

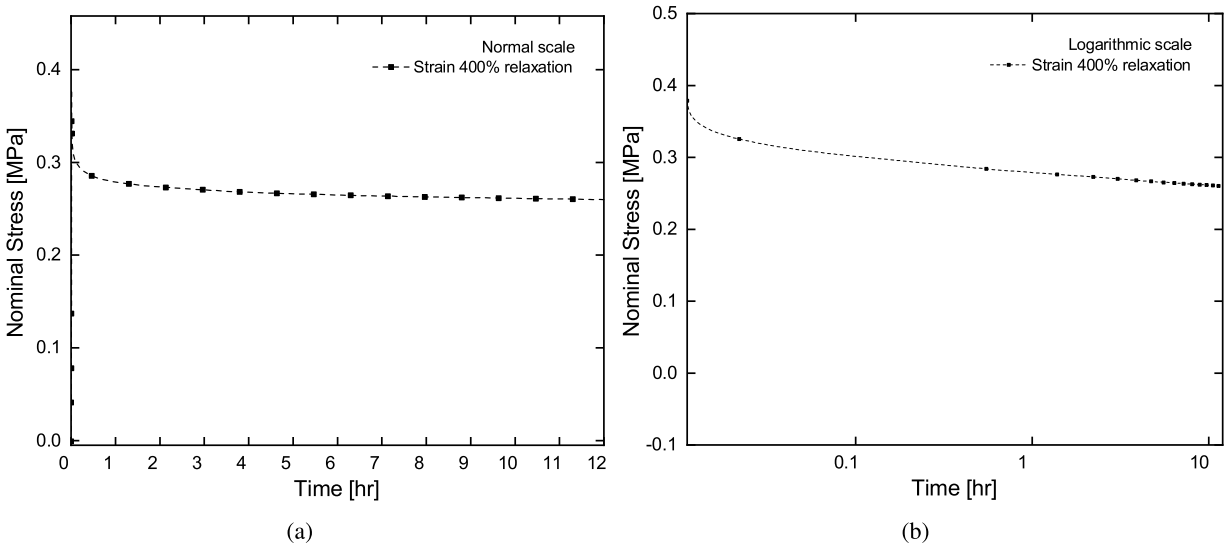

Fig. 10. A twelve-hour relaxation tests at strain 400%. (a) On a linear time axis, (b) on a logarithmic time axis.

with more cycles, the peak stress experiences a reduction and tends to stabilize as well. At a smaller maximum strain, the reduction is smaller and stabilizes at an earlier cycle. This pattern shares a resemblance to the relaxation behaviour. In fact, a stress relaxation undergoes during the loading and unloading processes. Hence, the peak stress decreases with repeated cycles. This behaviour is called the cyclic relaxation [17]. In contrast, the normal stress relaxation, where a specimen is held fixed after a certain strain, is called the static relaxation.

A test of multiple cycles with a 100% increment of strain is performed as is shown in Fig. 8. Therein, a curve of the single cycle test serves as an envelope of the curve of the multi-cycle test. Each of the reloading paths reaches the maximum stress of the former cycle. This characteristic is also evidence of the strain-induced softening and is a typical outcome of the Mullins effect [18–21,36].

Furthermore, it is observed that upon unloading, specimens come back to their original configurations, regardless of the strain level and the cycle count, as is shown in Fig. 9 in a close-up look. Even an unloading after the relaxation of several hours, the residual strain is negligible after the applied force is released. However, for a typical viscoelastic material, a recoverable residual strain exists right after an unloading since the strain and stress responses are not fully synchronized, which is not the case of Ecoflex.

3.3. Relaxation behaviour

Stress relaxation is one of the key phenomena to identify the time-dependent behaviour of any polymeric material. Firstly, a relaxation test is performed where a sample is elongated at strain 400% with the crosshead speed of 5 mm/s (close to the maximum of the machine) and let it relax. The test results are plotted on a linear time scale in Fig. 10(a) as well as in a logarithmic time scale in Fig. 10(b). The virgin material exhibits a significant stress relaxation behaviour. Note that even though it seems an equilibrium stress (the stress after the entire removal of the time-dependent portion) is reached under a linear time scale, a logarithmic time scale gives us a better picture that a declining trend still exists even after twelve hours of relaxation. Hence, a sample might take a longer time to reach the actual equilibrium stress. In the following section, all relaxation tests are plotted on a logarithmic time scale. Since there is only a small stress reduction between three and twelve hours of relaxations, for experimental simplicity, all relaxation experiments that follow hereafter will be carried out with a three-hour holding time.

Now more single-step relaxation tests on virgin Ecoflex specimens at strains from 100% to 500% with strain 100% interval are conducted. Fig. 11(a) illustrates the stress relaxations over the holding time on a logarithmic time scale, while Fig. 11(b) illustrates the same in a stress–strain format. As time evolves, the stress attenuates and tends to reach a stable value; the equilibrium stress. A larger strain results in a greater stress reduction from the peak stress to the equilibrium stress and a longer relaxation time to reach the equilibrium stress. At larger strains such as 400% and 500%, declining tendencies of the stresses still exist over three hours of relaxations. It means that the actual equilibrium stresses are smaller than the current relaxation stresses (the stress at the actual stage of relaxation time).

Given that the stress softening is significantly a strain-induced phenomenon for Ecoflex, as is mentioned in Section 3.2, few relaxation tests are carried out after several cycles of pre-stretch at various strains. In Fig. 12, all specimens are pre-stretched at a strain 500% for one cycle, and then they are allowed to relax at different strains starting from 100% up to 500%. Due to the 500% pre-stretch, the stress softening occurs prior to actual stress relaxations. For the tests from strains 100% to 400%, it can be observed that all the stresses only experience a minimal decrease where most of the stress drops happen within a few minutes. Even though we plot stress evolutions on the logarithmic time axis as in Fig. 12(a), there is only a slight declining tendency. After the pre-stretch at a larger strain and the consequent stress softening, most of the non-equilibrium stresses are almost removed. Additional tests over 400%, i.e., 450%, 475%, 500%, are also performed. For these cases, when the relaxation strain approaching the value of the pre-stretch, the influence of softening is less significant and the stress relaxation gets more pronounced.

Fig. 13(a) compares the relaxation stresses of the tests with and without the pre-stretch at a strain 500%. With an increase of the applied relaxation strain, the difference of relaxation stresses between the tests with and without a pre-stretch enlarges and then shrinks near the strain level of pre-stretch. This pattern is similar to the difference in the cyclic responses between a virgin and a pre-stretched specimens. A larger strain softening contributes to a lower relaxation stress. Fig. 13(b) compares the dissipation energy densities of the two tests. Here, the energy density is calculated by the closed area surrounded by the loading, relaxation and unloading path in the stress–strain curve of a relaxation test, such as Fig. 14. It can be seen that the hysteresis is removed significantly with a pre-stretch, similar to the results in multi-cyclic tests.

Since it is observed that the stress relaxation does not proceed fully at a plateau even after twelve hours of relaxation, the equilibrium stress is not fully identified. Bearing in mind that a pre-stretch can

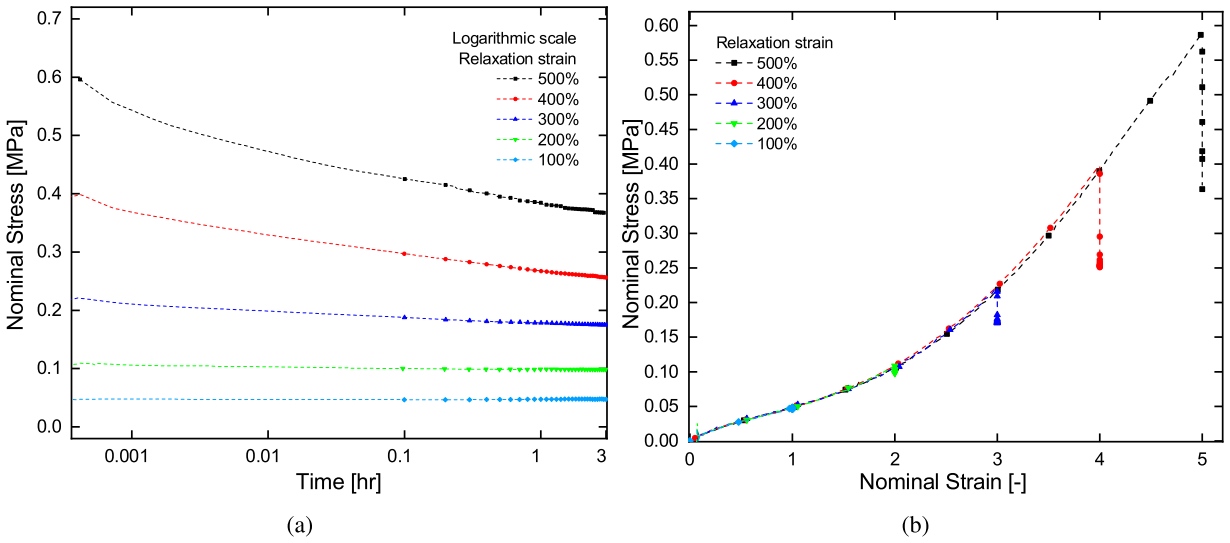

Fig. 11. Three-hour relaxation tests at different relaxation strains. (a) Stress evolution curves plotted on a logarithmic time axis, (b) stress–strain curves.

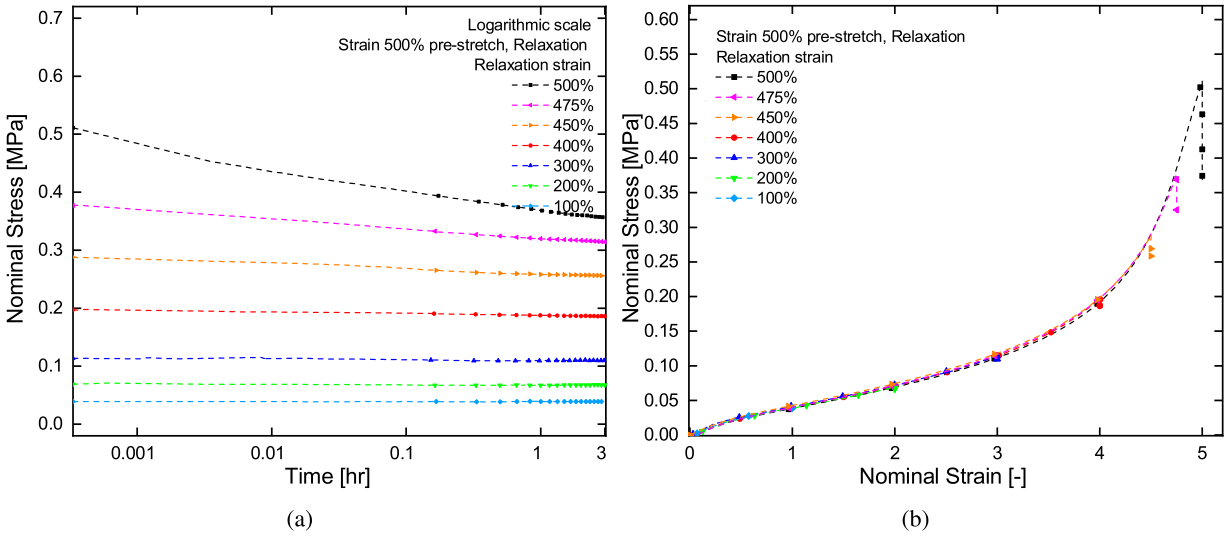

Fig. 12. Three-hour relaxation tests with a pre-stretch of strain 500% at different relaxation strains. (a) Stress evolution plotted on a logarithmic time axis, (b) stress–strain curves.

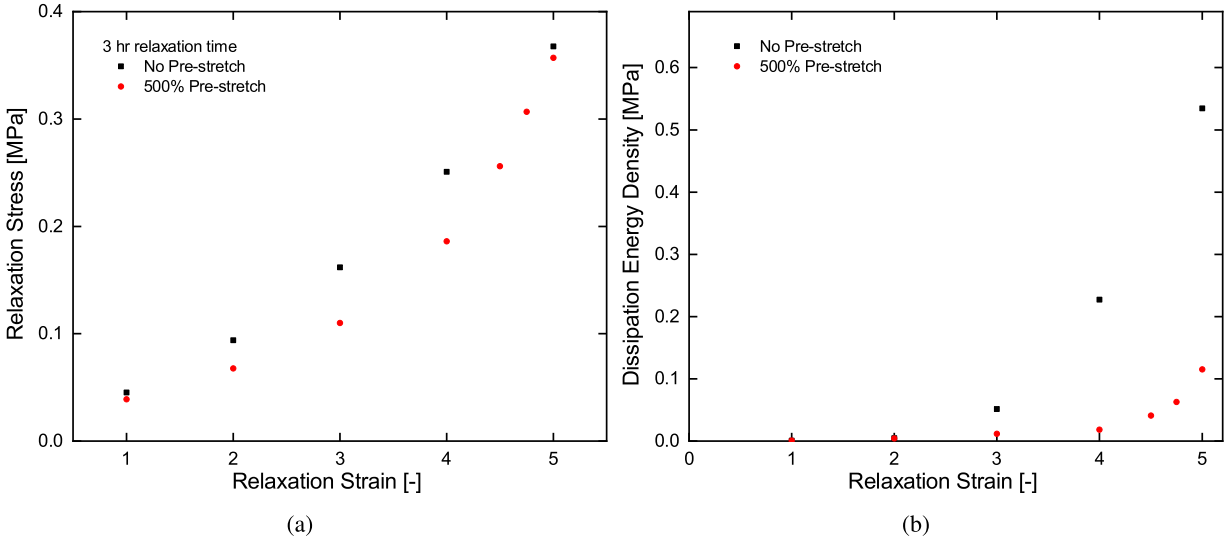

Fig. 13. Comparison between three-hour relaxation tests with and without a pre-stretch of strain 500%. (a) Relaxation stress at different relaxation strains, (b) dissipation energy density at different relaxation strains after unloading.

largely remove the relaxation behaviour, one may consider that the equilibrium stress may be achieved earlier by applying a larger pre-stretch without waiting for a long-time relaxation. On these grounds, relaxation tests with a cycle of pre-stretch at various strain levels larger than applied relaxation strains are carried out, see Fig. 15. By plotting the stress evolutions again on a logarithmic time axis, it is revealed that with a larger pre-stretch, a relaxation test begins with a low peak stress, and then the stress relaxes quickly to a lower level. However, from the tendency of these curves, a smaller pre-stretch retains a larger slope of the stress reduction, indicating that there is a possibility that after an infinite time period, all the stresses converge at the same value, i.e., the equilibrium stress, regardless of the strain level of the pre-stretch. Under such an assumption, the equilibrium stress is irrelevant to the pre-stretch level, and the softening caused by the pre-stretch takes the place of a portion of relaxation. A pre-stretch can simply be an easier way in obtaining the equilibrium stresses.

3.4. A comparison between stress softening and stress relaxation

From the aforementioned discussion, it is found that the strain-induced stress softening serves a role analogous to the relaxation to cause a stress decrease. A further demonstration can be made by a comparison between relaxation and softening responses in Fig. 16. A one cycle cyclic test at strain 320%, a relaxation test at strain 300%, and a cyclic test with one hundred cycles at 300% are carried out as pre-treatments on different specimens, as is shown in Fig. 16(a). These three different pre-treatments represent the larger strain softening, the static relaxation and the cyclic relaxation process. Then all the specimens are reloaded up to strain 500%. As is shown in Fig. 16(b), the responses almost evolve along the same path for three types of pre-treatments, which indicate a similar effect on the specimens' behaviour.

Therefore, the static and cyclic relaxation tests and the stress softening can be summarized as a time-dependent stress reduction process, and this process takes place in a so-called non-equilibrium stress portion in contrast to the time independent equilibrium stress portion. One may consider from a micro-physics perspective that these stress reductions could be caused by the same reason, such as breakage of chain bonds or disentanglements of the chain networks [22]. Note that while doing relaxation tests at large strains higher than 500%, many specimens failed in the middle after around ten minutes or less. A failure during relaxation is also observed in other tests such as [23]. This rather a surprising phenomenon that a relaxation test results in material failure could possibly be evidence of bonds breakage accumulation or disentanglement evolution during relaxation. The underlying micro-mechanics needs a further investigation.

3.5. Strain rate dependence

In the previous sections, the relaxation, a time-dependent phenomenon, is observed. Therefore, it can be envisaged that a strain rate-dependent phenomenon may also exist. In order to quantify the strain rate dependence of the polymer, load–unloading–reloading cyclic tests at different strain rates are carried out. It is interesting to note that virgin specimens clearly demonstrate strain rate dependence beyond strain 200%. For example, at strain 400% from 0.0001/s to 0.1/s strain rates with a four decades difference, the ultimate stress increases from 0.3 MPa to 0.4 MPa, see Fig. 17.

Fig. 18(a) shows that a higher strain rate brings a higher stress value in the first few cycles. However, with the increase of the number of cycles, the peak stress decreases quickly and tends to reach the same value as the ones of lower rates. This is again partially due to the cyclic relaxation response. Similar to the static relaxation, a higher strain rate only leads to a higher peak stress but a faster stress reduction and the same equilibrium stress. Fig. 18(b) shows that a higher strain rate leads to a larger hysteresis at the first cycle. Here, due to the softening

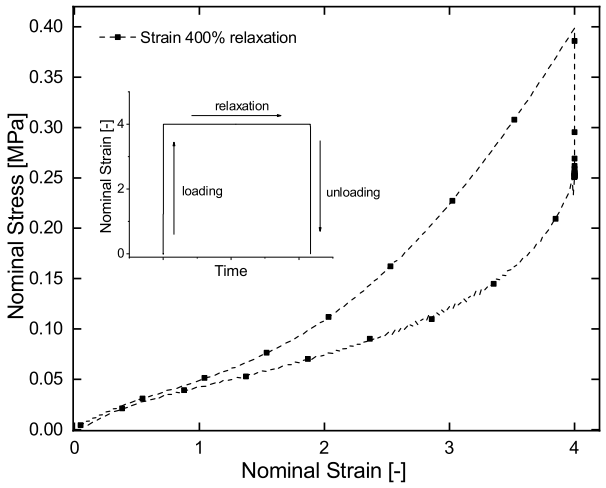

Fig. 14. A relaxation test with the unloading path.

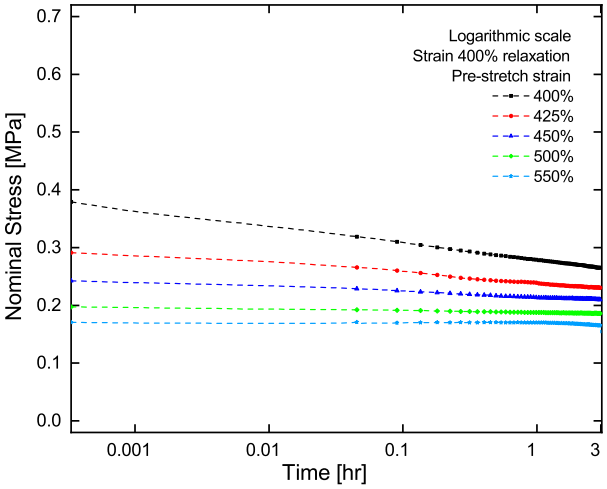

Fig. 15. Three-hour relaxation tests at strain 400% with different levels of pre-stretch.

behaviour, from the second cycles the dissipation energies are almost the same at different strain rates.

When the time-dependent non-equilibrium portion is removed by pre-treatments, the time or rate dependence behaviour will disappear right afterwards, as is mentioned in Section 3.3. In Fig. 19, two reloading curves at strain 400% with two different strain rates after three different types of pre-treatments are compared: a larger pre-stretch of 500% (Fig. 19(a)), a relaxation test at 400% (Fig. 19(b)), a strain with multiple cycles at 400% (Fig. 19(c)). Even though the strain rates in the graphs are 500 times, 400 times, and 100 times different, respectively, all two curves in each graph are almost overlapped. This result supports our assumption that the stress softening by loading–unloading cyclic tests, static and cyclic relaxations have the similar stress reduction effects. This fact also shows that after removal of the non-equilibrium stress by any of the three processes, the stress obtained does not depend on time. Hence, we can term the stress as the equilibrium one. Furthermore, for a viscoelastic material, in addition to the stress reduction induced by the relaxation during the loading path, a common phenomenon is that the stress increases during the strain holding period on an unloading path [24–26]. This phenomenon is not observed for the case of Ecoflex silicone rubber. Therefore, it can be concluded that Ecoflex does not demonstrate significant viscoelastic behaviour.

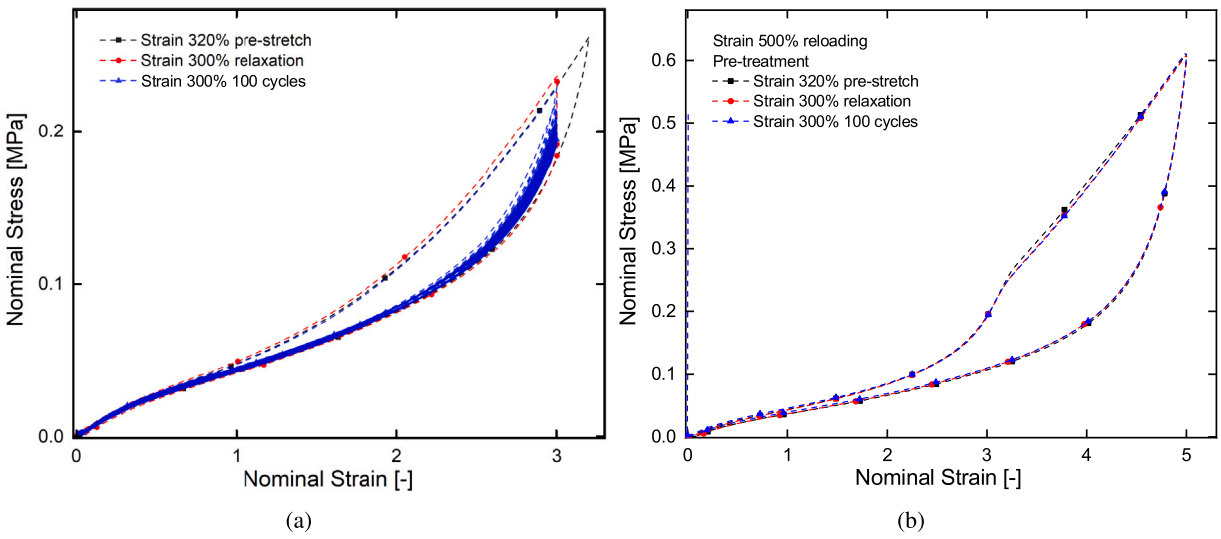

Fig. 16. Comparison between relaxation and softening responses. (a) A cyclic test at a strain 320% and a relaxation test with 100 cycles at strain 350%, (b) reloading tests to strain 500% of two tests in Fig. 16(a).

3.6. Temperature dependence

In the previous sections, we observe that the stress of the material consists of two parts: an equilibrium stress part and a non-equilibrium stress part. In this section, similar to the investigation of the strain rate dependence, the influences of temperature on these two stress portions are also tested, respectively. Several researches illustrate that mechanical properties of silicone polymers are sensitive to temperature variations [15,27,28]; although such types of dependence are not as pronounced as other polymers such as acrylics [29]. Therefore, we have conducted a couple of cyclic tests within the temperature chamber. Tests performed at different temperatures with a strain of 400% are presented in Fig. 20, which shows that the polymer is somehow temperature-sensitive. Before strain 250%, the stress values increase as the temperature increases, while over strain 250% the opposite trend is observed, i.e., the stress level decreases as the temperature increases. Moreover, the hysteresis decreases as the temperature increases.

Note that tests at 140 °C temperature undergo failures in the gauge section of the specimen with a good reproducibility. Due to the displacement limit of the machine while tests are being performed within the temperature chamber, it is a challenging task to perform failure tests with a larger ultimate extension at a lower temperature. Nevertheless, these results give us a glimpse of the fact that the material failure is also dependent on temperature, and it could be predicted that a higher temperature leads to a smaller ultimate extension before a failure.

In order to see what exactly happens to the non-equilibrium stress portion, the equilibrium stress portion should closely be monitored too. Fig. 21 illustrates the tests at different temperatures and at a strain of 400% with a 500% pre-stretch. It can be seen that the hysteresis is almost removed. From a lower temperature to ambient and then to elevated temperature, the stress level undergoes a progressive increase. Note that in Section 3.2, it is found that the hysteresis is small before strain 200%, indicating that the equilibrium stress plays a dominant part at this strain range. This explains the increase of stress with the increasing temperature of total stress. After strain 250% or so, the time-dependent non-equilibrium stress overtakes the equilibrium stress. Therefore, the total stress exhibits a decreasing trend at a higher temperature. Finally, it can be concluded that with the temperature increasing, the equilibrium stress increases and the non-equilibrium stress decreases.

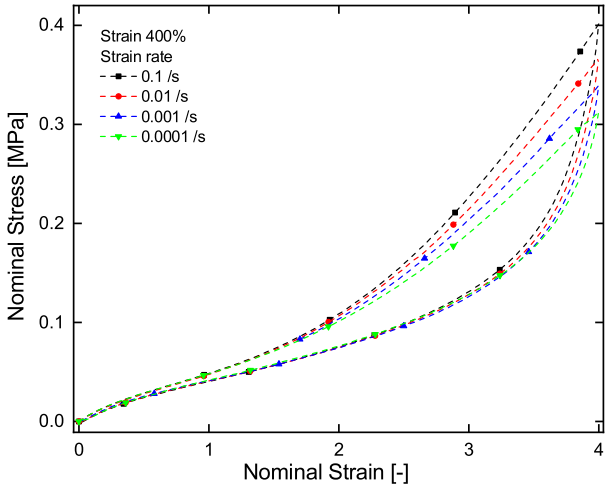

Fig. 17. Cyclic tests at different strain rates with a strain 400%.

3.7. Stress recovery

Although many soft materials exhibit a similar stress softening behaviour as Ecoflex silicone rubbers described in the previous sections, the extent of stress recovery varies from material to material [19,22,30–33]. In this section, the recovery behaviour of Ecoflex is investigated in detail.

In Fig. 22, the stress recovery behaviour is depicted. All specimens are pre-stretched beforehand, and then each specimen is reloaded after different recovery times at a stress-free state. Fig. 22(a) shows that the stress level of the first reloading cycle increases along the loading path with a longer recovery period. This indicates that the stress softened in the non-equilibrium portion will recover as time passes. The recovery can also be evaluated by the hysteresis (calculated as dissipation energy density) and the hysteresis ratio between the first loading and the reloading (the ratio of dissipation energy density). Note that the dissipation energy density for the first loading cycle of a virgin specimen is 0.2055 MPa. The result is presented in Fig. 22(b), where the left axial depicted the energy density and the right axial depicted the energy density ratio. The hysteresis recovers with time and continuously maintains an increasing trend, although after a month it is still far from that of a virgin specimen. Some researches suggest that

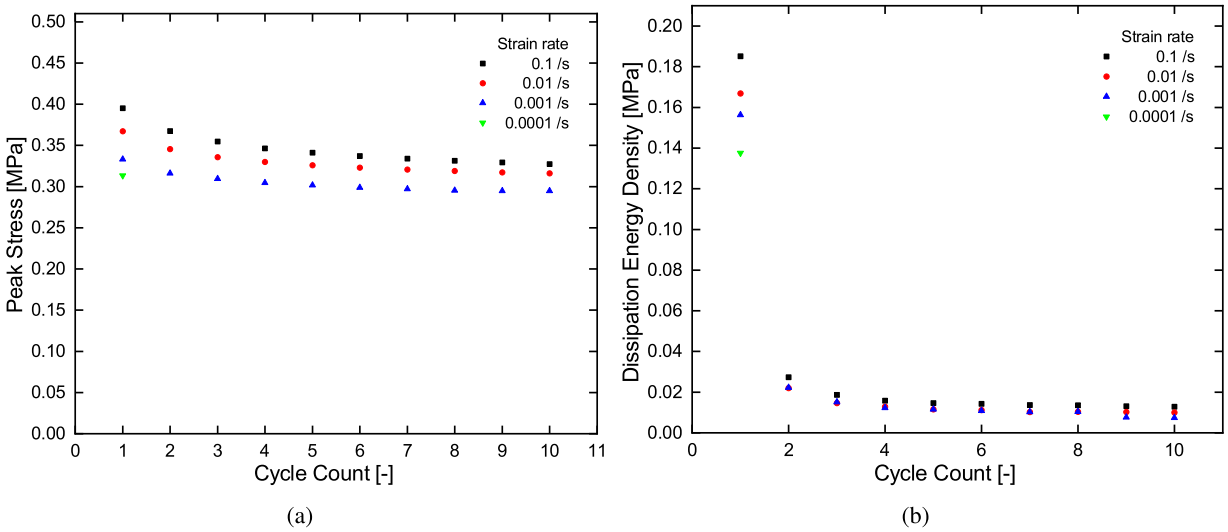

Fig. 18. Peak stress and dissipation energy density of cyclic tests at different strain rates with multiple cycles. (a) Peak stress versus cycle count, (b) dissipation energy density versus cycle count.

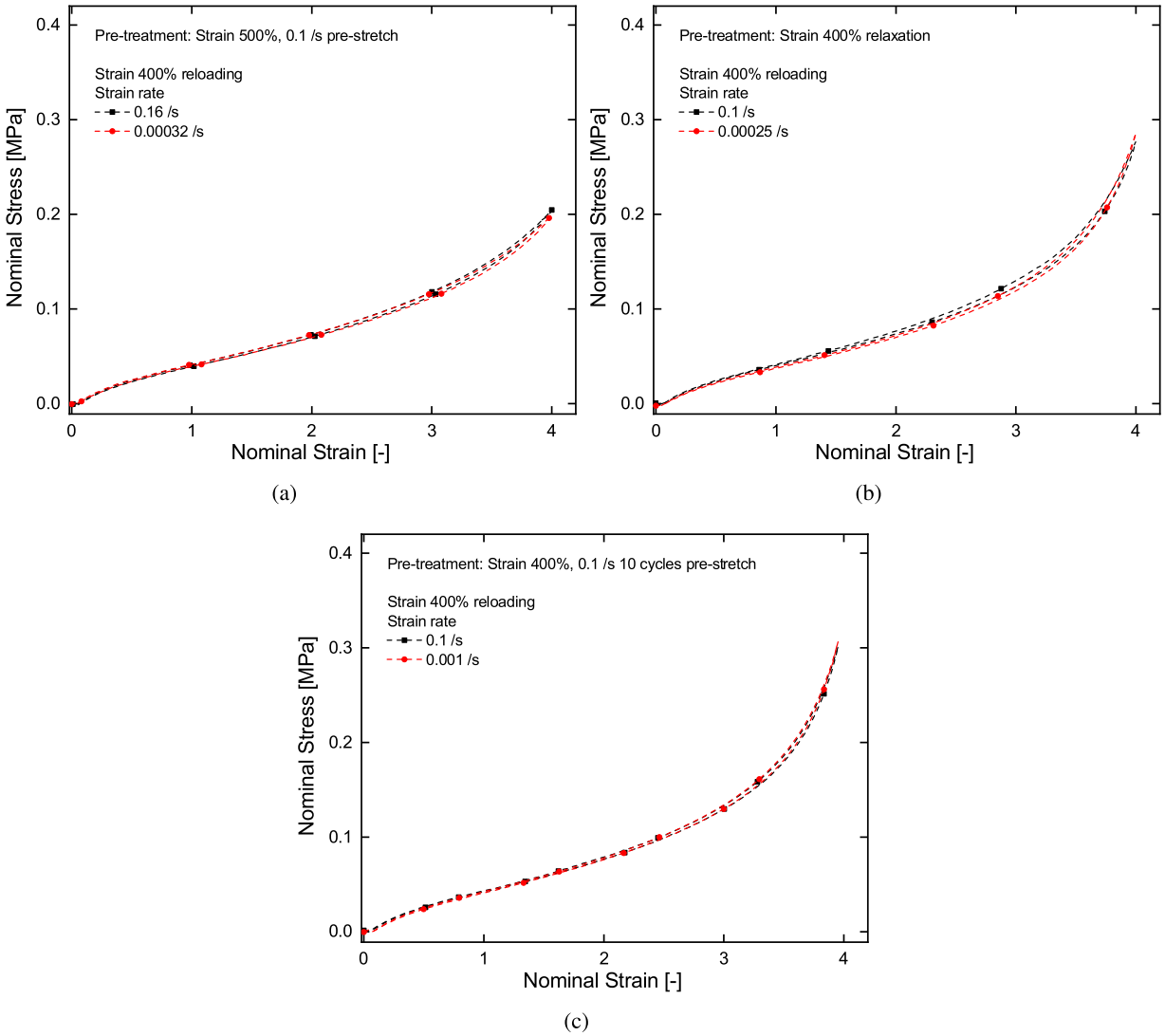

Fig. 19. Cyclic tests at different strain rates after different types of pre-treatments. (a) Pre-stretch at strain 500%, (b) relaxation at strain 400%, (c) ten cycles pre-stretch at strain 400%.

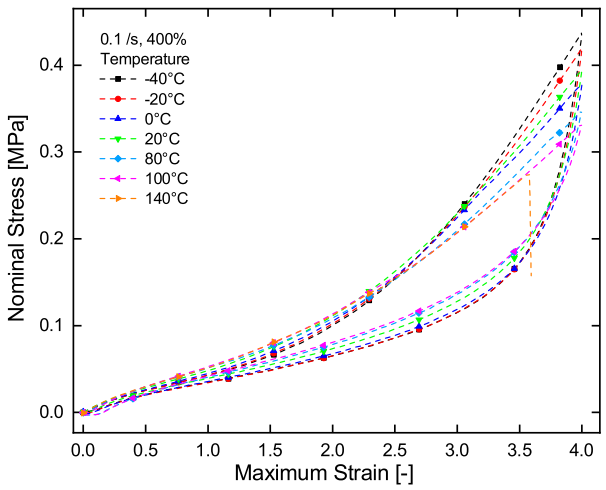

Fig. 20. Cyclic tests at various temperatures at a strain 400%.

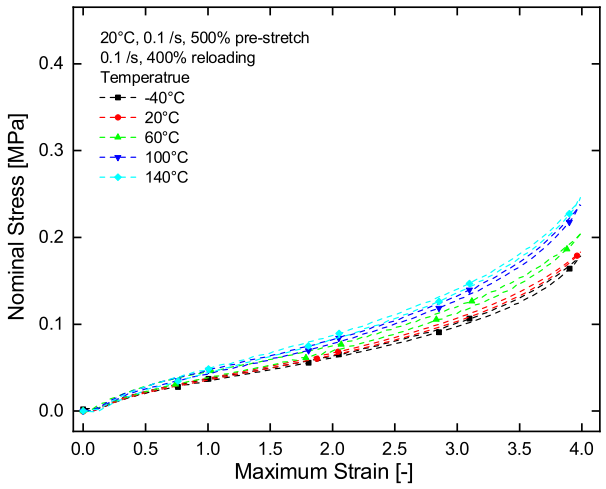

Fig. 21. Cyclic tests at various temperatures for a strain 400% where the pre-stretch is conducted at room temperature with a strain of 500%.

such softening is partly recoverable and partly unrecoverable [22,32,33]. However, there is also a possibility for Ecoflex that the hysteresis reduction and stress reduction can recover fully after 'a sufficient long time'.

Since we have presumed that the stress relaxation imposes similar influences on Ecoflex as the stress softening, one can predict that the relaxation could also recover with time. In a relaxation test of the material, stress decreases significantly. The immediate reloading curve is also close to the unloading path right after relaxation in Fig. 23(a). After recovery for a week, the hysteresis of the reloading cycle shows obvious recovery. It is also illustrated in Fig. 23(b). It can also be observed that with time increases, the stress level at loading and unloading paths and the peak stress will recover to a certain degree, which is similar to the recovery after the stress softening. Overall, a major stress recovery is witnessed in the non-equilibrium portion of the stress after any type of stress reduction.

4. Conclusions

In this study, we focus on the characterization of the thermo-mechanical behaviour of a widely used silicone rubber, i.e., Ecoflex of Shore 00-30. A comprehensive and systematical mechanical experimentation is carried out including cyclic loading–unloading tests with multiple cycles, relaxation tests, reloading tests after recovery, strain rate and temperature dependence tests. After a rigorous study on Ecoflex, following summary can be drawn:

- A significant strain-induced stress softening phenomenon is observed. A time-dependent relaxation behaviour is also observed. It is found that any pre-treatments either by applying multiple cycles or a pre-stretching at a higher strain, or relaxing the specimen at a specific strain can cause a significant stress decrease and the removal of hysteresis. The corresponding stress softening and relaxation share a similarity on the material response, and they may be attributed to some micro-mechanical causes such as polymer chain breakages.
- Based on the experimental results, it is assumed that the total stress could be decomposed into two parts: an equilibrium stress portion that is time-independent, and a non-equilibrium stress portion which is time-dependent.
- The non-equilibrium stress portion can be removed by stress softening, static relaxation or cyclic relaxation. This portion is significantly recoverable with time. A possibility is that all the stress softened or relaxed in this non-equilibrium portion could recover completely after a long enough time under a stress-free state.

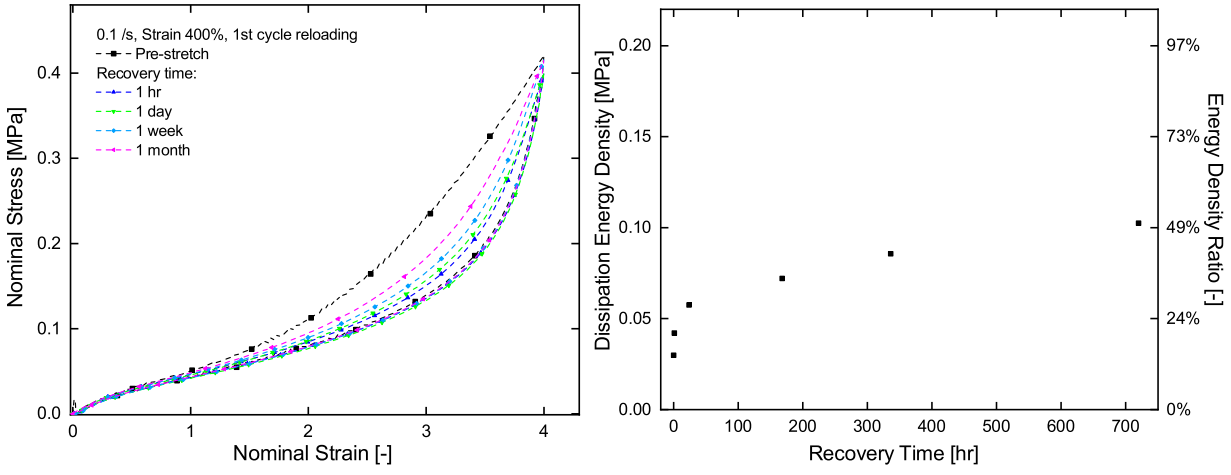

Fig. 22. Reloading of pre-stretched specimens after different recovery periods. (a) Stress–strain curves, (b) dissipation energy density.

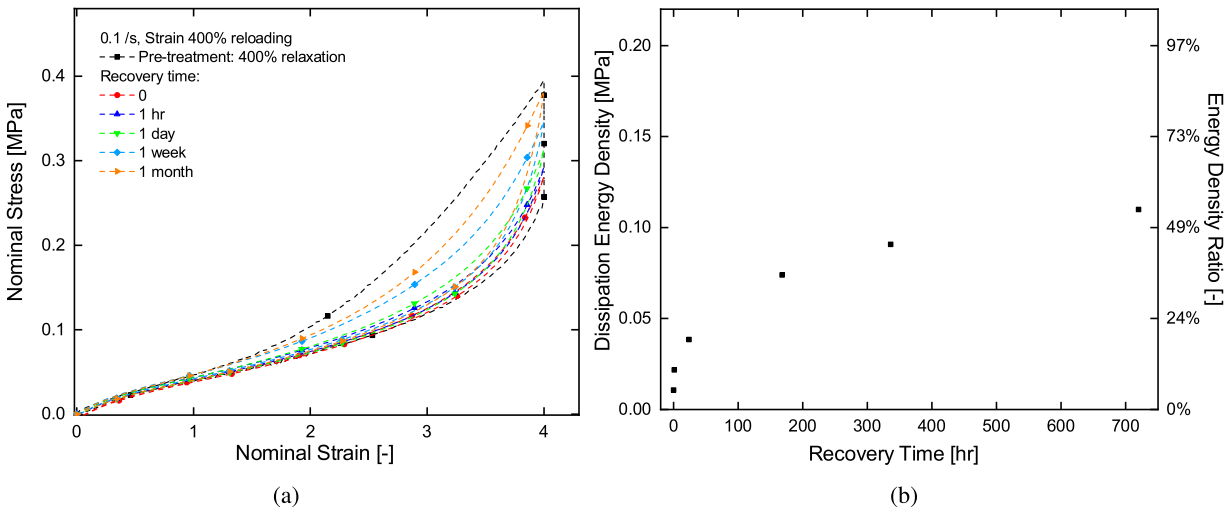

Fig. 23. Reloading of relaxed specimens after different recovery periods. (a) Stress–strain curves of relaxation and reloading, (b) dissipation energy density of reloading.

- No residual strain is observed, and no pronounced strain rate dependence is found after the removal of the non-equilibrium stress portion. This implies that the material may not be a typical viscoelastic polymer.
- Temperature dependence is observed to some extends. The equilibrium stress increases as temperature increases, while the non-equilibrium stress and the consequent hysteresis decrease as the temperature increases.

In a separate contribution [34], we characterize Ecoflex of other Shore hardnesses using similar protocols illustrated in this study. Furthermore, we are working to develop constitutive models that can capture the time-dependent stress softening and recovery behaviour of Ecoflex.

Declaration of competing interest

The authors declare that they have no known competing financial interests or personal relationships that could have appeared to influence the work reported in this paper.

Acknowledgements

The first two authors would like to extend their sincere appreciation to Zienkiewicz Centre for Computational Engineering (ZCCE), Swansea University, UK for supporting the work. This support facilitates an exchange visit of the first author to ZCCE. This work is partially supported by the National Science Fund for Distinguished Young Scholars (No.11925203) and the National Natural Science Foundation of China (No.1672110). The work is also benefited from the Fundamental Research Funds for the Central Universities, SCUT (2018PY21).

References

[1] S. Zakaria, L. Yu, G. Kofod, A.L. Skov, The influence of static pre-stretching on the mechanical ageing of filled silicone rubbers for dielectric elastomer applications, Mater. Today Commun. 4 (2015) 204–213, http://dx.doi.org/10.1016/j.mtcomm.2015.08.002.

[2] L. Bernardi, R. Hopf, A. Ferrari, A. Ehret, E. Mazza, On the large strain deformation behavior of silicone-based elastomers for biomedical applications, Polym. Test. 58 (2017) 189–198, http://dx.doi.org/10.1016/j.polymertesting.2016.12.029.

[3] L. Bernardi, R. Hopf, D. Sibilio, A. Ferrari, A. Ehret, E. Mazza, On the cyclic deformation behavior, fracture properties and cytotoxicity of silicone-based elastomers for biomedical applications, Polym. Test. 60 (2017) 117–123, http://dx.doi.org/10.1016/j.polymertesting.2017.03.018.

[4] J.S. Bergstroem, Large Strain Time-Dependent Behavior of Elastomeric Materials (Ph.D. dissertation), Massachusetts Institute of Technology, USA, 1999.

[5] H. Hoeksema, M.D. Vos, J. Verbelen, A. Pirayesh, S. Monstrey, Scar management by means of occlusion and hydration: A comparative study of silicones versus a hydrating gel-cream, Burns 39 (7) (2013) 1437–1448, http://dx.doi.org/10.1016/j.burns.2013.03.025.

[6] M. Mehnert, M. Hossain, P. Steinmann, Numerical modeling of thermo-electro-viscoelasticity with field-dependent material parameters, Int. J. Non-Linear Mech. 106 (2018) 13–24, http://dx.doi.org/10.1016/j.ijnonlinmec.2018.08.016.

[7] L. Guo, Y. Lv, Z. Deng, Y. Wang, X. Zan, Tension testing of silicone rubber at high strain rates, Polym. Test. 50 (2016) 270–275, http://dx.doi.org/10.1016/j.polymertesting.2016.01.021.

[8] M. Amjadi, Y.J. Yoon, I. Park, Ultra-stretchable and skin-mountable strain sensors using carbon nanotubes–Ecoflex nanocomposites, Nanotechnology 26 (37) (2015) 375501, http://dx.doi.org/10.1088/0957-4484/26/37/375501.

[9] J.L. Sparks, N.A. Vavalle, K.E. Kasting, B. Long, M.L. Tanaka, P.A. Sanger, K. Schnell, T.A. Conner-Kerr, Use of silicone materials to simulate tissue biomechanics as related to deep tissue injury, Adv. Skin Wound Care 28 (2) (2015) 59–68, http://dx.doi.org/10.1097/01.asw.0000460127.47415.6e.

[10] M. Hossain, D.K. Vu, P. Steinmann, Experimental study and numerical modelling of VHB 4910 polymer, Comput. Mater. Sci. 59 (2012) 65–74, http://dx.doi.org/10.1016/j.commatsci.2012.02.027.

[11] M. Johlitz, H. Steeb, S. Diebels, A. Chatzouridou, J. Batal, W. Possart, Experimental and theoretical investigation of nonlinear viscoelastic polyurethane systems, J. Mater. Sci. 42 (23) (2007) 9894–9904, http://dx.doi.org/10.1007/s10853-006-1479-4.

[12] Z. Liao, M. Hossain, X. Yao, M. Mehnert, P. Steinmann, On thermo-viscoelastic experimental characterization and numerical modelling of VHB polymer, Int. J. Non-Linear Mech. 118 (2020) 103263, http://dx.doi.org/10.1016/j.ijnonlinmec.2019.103263.

[13] M. Wissler, E. Mazza, Mechanical behavior of an acrylic elastomer used in dielectric elastomer actuators, Sensors Actuators A 134 (2) (2007) 494–504, http://dx.doi.org/10.1016/j.sna.2006.05.024.

[14] R. Sahu, K. Patra, J. Szpunar, Experimental study and numerical modelling of creep and stress relaxation of dielectric elastomers, Strain 51 (1) (2014) 43–54, http://dx.doi.org/10.1111/str.12117.

[15] T. Rey, G. Chagnon, J.-B.L. Cam, D. Favier, Influence of the temperature on the mechanical behaviour of filled and unfilled silicone rubbers, Polym. Test. 32 (3) (2013) 492–501, http://dx.doi.org/10.1016/j.polymertesting.2013.01.008.

[16] G. Chagnon, On the relevance of continuum damage mechanics as applied to the Mullins effect in elastomers, J. Mech. Phys. Solids 52 (7) (2004) 1627–1650, http://dx.doi.org/10.1016/j.jmps.2003.12.006.

[17] G. Weng, Cyclic stress relaxation of polycrystalline metals at elevated temperature, Int. J. Solids Struct. 19 (6) (1983) 541–550, http://dx.doi.org/10.1016/0020-7683(83)90091-4.

[18] I. Stevenson, L. David, C. Gauthier, L. Arambourg, J. Davenas, G. Vigier, Influence of SiO_2 fillers on the irradiation ageing of silicone rubbers, Polymer 42 (22) (2001) 9287–9292, http://dx.doi.org/10.1016/s0032-3861(01)00470-0.

[19] D.E. Hanson, M. Hawley, R. Houlton, K. Chitanvis, P. Rae, E.B. Orler, D.A. Wrobleski, Stress softening experiments in silica-filled polydimethylsiloxane provide insight into a mechanism for the Mullins effect, Polymer 46 (24) (2005) 10989–10995, http://dx.doi.org/10.1016/j.polymer.2005.09.039.

[20] A. Dorfmann, R. Ogden, A constitutive model for the Mullins effect with permanent set in particle-reinforced rubber, Int. J. Solids Struct. 41 (7) (2004) 1855–1878, http://dx.doi.org/10.1016/j.ijsolstr.2003.11.014.
[21] S. Wang, S.A. Chester, Experimental characterization and continuum modeling of inelasticity in filled rubber-like materials, Int. J. Solids Struct. 136–137 (2018) 125–136, http://dx.doi.org/10.1016/j.ijsolstr.2017.12.010.
[22] J. Diani, B. Fayolle, P. Gilormini, A review on the Mullins effect, Eur. Polym. J. 45 (3) (2009) 601–612, http://dx.doi.org/10.1016/j.eurpolymj.2008.11.017.
[23] C.G. Skamniotis, M. Elliott, M.N. Charalambides, On modeling the large strain fracture behaviour of soft viscous foods, Phys. Fluids 29 (12) (2017) 121610, http://dx.doi.org/10.1063/1.4993754.
[24] A. Lion, A constitutive model for carbon black filled rubber: Experimental investigations and mathematical representation, Contin. Mech. Thermodyn. 8 (3) (1996) 153–169, http://dx.doi.org/10.1007/bf01181853.
[25] J.S. Bergstroem, M.C. Boyce, Constitutive modeling of the large strain time-dependent behavior of elastomers, J. Mech. Phys. Solids 46 (5) (1998) 931–954, http://dx.doi.org/10.1016/S0022-5096(97)00075-6.
[26] H. Qi, M. Boyce, Stress–strain behavior of thermoplastic polyurethanes, Mech. Mater. 37 (8) (2005) 817–839, http://dx.doi.org/10.1016/j.mechmat.2004.08.001.
[27] L. Guo, Y. Wang, High-rate tensile behavior of silicone rubber at various temperatures, Rubber Chem. Technol. (2019) http://dx.doi.org/10.5254/rct.19.81562, in press.
[28] X. Li, T. Bai, Z. Li, L. Liu, Influence of the temperature on the hyper-elastic mechanical behavior of carbon black filled natural rubbers, Mech. Mater. 95 (2016) 136–145, http://dx.doi.org/10.1016/j.mechmat.2016.01.010.
[29] Z. Liao, X. Yao, L. Zhang, M. Hossain, J. Wang, S. Zang, Temperature and strain rate dependent large tensile deformation and tensile failure behavior of transparent polyurethane at intermediate strain rates, Int. J. Impact Eng. 129 (2019) 152–167, http://dx.doi.org/10.1016/j.ijimpeng.2019.03.005.
[30] Z. Rigbi, Reinforcement of rubber by carbon black, in: Properties of Polymers, Springer Berlin Heidelberg, 2005, pp. 21–68, http://dx.doi.org/10.1007/3-540-10204-3_2.
[31] L. Yan, D.A. Dillard, R.L. West, L.D. Lower, G.V. Gordon, Mullins effect recovery of a nanoparticle-filled polymer, J. Polym. Sci. B 48 (21) (2010) 2207–2214, http://dx.doi.org/10.1002/polb.22102.
[32] S. Wang, S.A. Chester, Modeling thermal recovery of the Mullins effect, Mech. Mater. 126 (2018) 88–98, http://dx.doi.org/10.1016/j.mechmat.2018.08.002.
[33] J. Plagge, M. Klueppel, Mullins effect revisited: Relaxation, recovery and high-strain damage, Mater. Today Commun. 20 (2019) 100588, http://dx.doi.org/10.1016/j.mtcomm.2019.100588.
[34] Z. Liao, M. Hossain, X. Yao, Ecoflex polymer of different shore hardnesses: Experimental investigations and constitutive modelling, Mech. Mater. 114 (2020) 103366, http://dx.doi.org/10.1016/j.mechmat.2020.103366.
[35] L. Mullins, Softening of rubber by deformation, Rubber Chem. Technol. 42 (1) (1969) 339–362, http://dx.doi.org/10.5254/1.3539210.
[36] L. Mullins, N.R. Tobin, Theoretical model for the elastic behavior of filler-reinforced vulcanized rubbers, Rubber Chem. Technol. 30 (2) (1957) 555–571, http://dx.doi.org/10.5254/1.3542705.